

Bioprinting with Live Cells

S. Burce Ozler, Can Kucukgul and Bahattin Koc

1 Introduction

The loss or failure of an organ or tissue is one of the most devastating, and costly problems in health care. The current treatment methods for organ/tissue loss or failure include transplantation of organs, surgical reconstruction, use of mechanical devices, or supplementation of metabolic products. Due to the growing need for organ transplantation and a lack of donor organs, tissue or organ engineering has progressed as a multidisciplinary field combining life sciences and engineering principles to restore, maintain, or improve function of tissues or organs [1, 2].

Traditionally, tissue engineering strategies are based on the cell seeding into synthetic, biological or composite scaffolds providing a suitable environment for cell attachment, proliferation and differentiation. A scaffold is highly porous complex structure providing an interconnected network that is designed to act as an artificial extracellular matrix (ECM) until the cells form their own ECM. In scaffold-based tissue engineering, three steps must be followed including finding a source of precursor cells from the patient, seeding these cells in vitro into the desired places of scaffold and surgically implanting the scaffold into the patient [3]. Scaffolds have been used to fabricate various tissue grafts including skin, cartilage, bone, blood vessels, bladder and myocardium [4–12]. Bioengineered tissue scaffolds attempt to mimic both the external shape and internal architecture of the replaced tissues.

The modeling of scaffolds has a great impact on the growth and proliferation of cells and a spatially and temporally controlled scaffold design could improve cell growth and differentiation [13]. Although many different scaffold manufacturing techniques such as salt-leaching, porogen melting, gas foaming, electrospinning,

B. Koc (✉) · S. B. Ozler · C. Kucukgul
Department of Manufacturing and Industrial Engineering,
Sabanci University, Istanbul, Turkey e-mail:
bahattinkoc@sabanciuniv.edu

© Springer International Publishing Switzerland 2016

1

K. Turksen (eds.), *Bioprinting in Regenerative Medicine*,
Stem Cell Biology and Regenerative Medicine, DOI 10.1007/978-3-319-21386-6_3

25 fiber deposition, molding and freeze-drying have been investigated in the past, it is 26
challenging to control pore size, porosity, pore interconnectivity and external geom27 etries
of scaffolds. In recent years, various additive manufacturing based methods 28 such as
bioplotting, bioprinting, ink-jet printing and stereolithography have been

29 used for biomanufacturing of complex three-dimensional (3D) tissue scaffolds to
30 overcome the limitations of conventional tissue engineering methods [14]. These 31
additive manufacturing based techniques allow to fabricate scaffolds layer-by-layer
32 with controlled external and internal geometries based on computer-aided models
33 of targeted tissues [15]. Several researchers have investigated designing function34 ally
gradient porous scaffolds with controllable variational pore size and heteroge35 neous porous
architecture [16, 17].

36 In scaffold-based tissue engineering, different biomaterials are used for scaffold 37
fabrication such as porous materials composed of biodegradable polymers (polylac38 tic acid,
polyglycolic acid, hyaluronic acid and several copolymers), hydroxyapatite 39 or calcium
phosphate-based materials and soft materials like collagens, fibrin, and 40 various hydrogels.
Although there is a plenty of choice for scaffold materials, an 41 ideal biomaterial for scaffold
fabrication should be nontoxic, nonimmunogenic, ca42 pable of maintaining mechanical
integrity for tissue growth and differentiation with 43 controlled degradation [3].

44 After implantation of a scaffold, it should degrade in a controlled manner and 45 the seeded
cells should proliferate and migrate into scaffold to replace the scaffold 46 biomaterial.
Newly-formed extracellular matrix (ECM) fills the places which were
47 previously occupied by the biomaterial of scaffolds. However, there are some draw48 backs
to create tissues with biodegradable scaffolds. Mostly, oxygen/nutrient deliv49 ery and
removal of metabolic waste are insufficient through the micro-channels of 50 a scaffold.
Additionally, biodegradation of the scaffold induces inflammation. Even 51 though the
biomaterials used may not be directly toxic, they can be metabolized to 52 toxic byproducts
[18].

53 Because of the above mentioned drawbacks, the recent tissue engineering studies 54 tend
towards ‘scaffold-free’ techniques. During the embryonic maturation, tissues 55 and organs
are formed without the need for any scaffolds [19, 20]. The self-assem56 bly and self-
organizing capabilities of cells and tissues are main driver for the field 57 of scaffold-free
tissue engineering. Self-assembly based tissue engineering aims to 58 produce fully biological
tissues with specific compositions and shapes having the 59 ability to grow their own ECM,
and therefore to reduce the immunogenic reactions 60 and other unpredicted complications
based on the use of scaffolds [21].

61 One way of implementing the self-assembly approach is the cell sheet technol62 ogy, which
has been applied clinically for the repair of skin, cornea, blood vessels, 63 and cardiomyocyte
patches to repair partial heart infarcts [18, 22, 23]. Another self64 assembly-based approach

is founded on the recognition that ‘nature knows best’. This approach relies on the principle that cell aggregates can be used as building blocks, since they have the intrinsic capacity to fuse together, known as tissue fluidity and self-assemble through morphogenetic processes if they are deposited in

close spatial organization [24–26]. The engineering of 3D living structures supported by the self-assembly and self-organizing capabilities of cells is commonly termed ‘bioprinting’. Bioprinting is an extension of tissue engineering, where the cells are delivered through the application of additive manufacturing techniques [27, 28]

This chapter focuses on scaffold-free tissue engineering and its adaptation to the technology of three dimensional bioprinting. Further, the importance as well as the challenges for 3D bioprinting using stem cells will be discussed in this chapter.

2 Bioprinting with Live Cells

2.1 2D Patterning and Cell-Sheet Technology

Placing cells into special patterns using the laser light has been one of the first methods used for 2D cell patterning [14]. These laser-based techniques utilize transparent ribbons on which one side is coated with cells that are either adhered to a biological polymer through initial cellular attachment or uniformly suspended in a thin layer of liquid or a hydrogel. A pulsed laser beam is transmitted through the ribbon and is used to push cells from the ribbon to the receiving substrate which is coated with hydrogels.

While laser based approaches enable to pattern living cells on a substrate and to layer multiple cell types, laser-based techniques have been also explored for positioning of cells in microarrays [32]. The resolution of laser-assisted bioprinting is affected by different factors such as the laser fluence, the wettability of the substrate, and the thickness and the viscosity of the biological layer [33]. Guilot and his group studied the effect of the viscosity of the bioink, laser energy, and laser printing speed on the resolution of cell printing [34] as shown in Fig. 1.

By using this method, various cell types including human osteosarcoma, rat cardiac cells and human umbilical vein endothelial cells (HUVEC) could be printed with micrometer accuracy on Matrigel as the absorptive layer [31, 35, 36]. More recently, the biological laser printing was used to print sodium alginate, nano-sized hydroxyapatite (HA) and human endothelial cells [37]. However, most of these methods are limited to two-dimensional patterning and it is difficult to fabricate three-dimensional tissue constructs because of process-induced cell injury. The thermal stress and ultraviolet radiation caused by laser printing could also affect

the cell viability.

105

Similar to 2D patterning, cell sheet technology is another scaffold-free method for construction of 2D and 3D engineered tissues. In this method, cells can be moved from a culture dish as a relatively stable confluent monolayer sheet without destroying cell-cell contacts. In order to build a substantial 3D tissue volume, many sheets need to be culminated in high amount of cells which requires vascularization for cell viability [15].

L'Heureux and his group produced a tissue engineered blood vessel using a cell sheet approach based on cultured human cells. The developed vessel contained all three histological layers such as the endothelium, the media and the adventitia. In

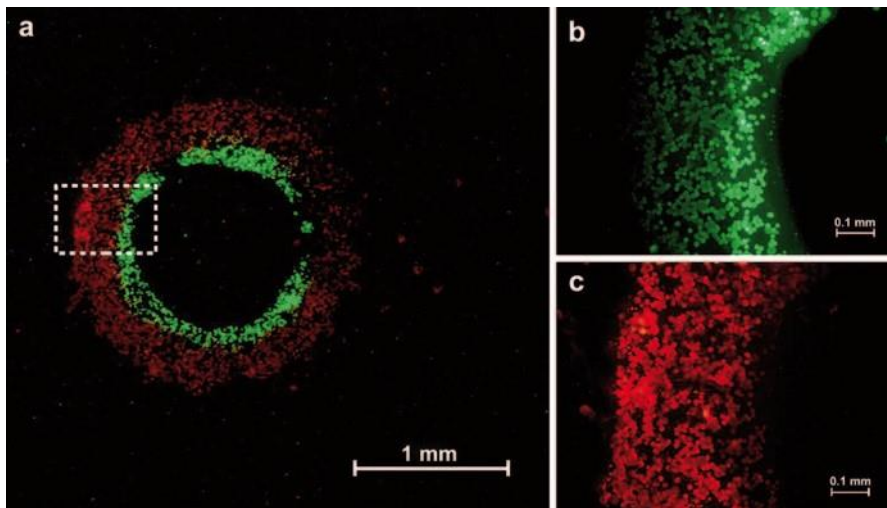


Fig. 1 Laser-assisted sequential two color cell printing in 2D. **a** The two cell suspensions (6·10⁷ cells/ml in DMEM, supplemented with 1% (w/v) alginate) were then printed according to a pattern of concentric circles). **b** Green Calcein stained cells within the region of interest as defined in **1a** (dashed rectangle). **c** Red fluorescent Dil-LDL stained cells within the same region of interest. (Adapted from [34])

¹¹⁴ this self-assembly approach, smooth-muscle cells and fibroblasts were cultured in ¹¹⁵ medium containing serum and ascorbic acid and produced their own extracellular ¹¹⁶ matrix (ECM). The smooth-muscle cell sheet was placed around a tubular mandrel ¹¹⁷ to produce the media of the vessel. A similar fibroblast cell sheet was wrapped ¹¹⁸ around the media to provide the adventitia after 8 weeks of maturation. Finally, ¹¹⁹ the tubular support was removed and endothelial cells were seeded in the lumen ¹²⁰ to form the endothelium. The tissue engineered blood vessel has burst strength of ¹²¹ over 2500 mm Hg which is significantly higher than that of human saphenous veins ¹²² (1680 ± 307 mm Hg) [23]. Sheet-based tissue engineering has been used by the same ¹²³ group to produce tissue engineered blood vessel (TEBV) suitable for autologous ¹²⁴ small diameter arterial revascularization in adult patients. Fibroblasts were cultured ¹²⁵ in conditions promoting

extracellular matrix (ECM) deposition to produce a cohesive sheet that can be detached from the culture flask. This approach also eliminates the use of smooth-muscle cells, whose early senescence is related with decreased burst pressures in human models. The decellularized internal membrane (IM) and living adventitia were assembled by wrapping fibroblast sheets around a temporary Teflon coated stainless steel support tube. After weeks-long maturation and dehydration to form an acellular substrate, the steel tube was removed and endothelial cells were seeded in the lumen of living TEVB. The transplantation of these blood vessels into dogs demonstrated good handling, suturability by the use of conventional surgical techniques. Ultimately, this is an effective approach to produce a completely biological and clinically applicable TEVB in spite of its relatively long production time (≈ 28 weeks) which clearly prevents its urgent clinical use [22].

Okano and colleagues have engineered a long-lasting cardiac tissue based on a similar self-assembled sheet based approach. In their method, culture dishes are first coated with a temperature-responsive polymer, poly (N-isopropylacrylamide)

(PIPAAM). The surface is relatively hydrophobic at 37°C allowing cells to attach and proliferate, while cooling below 32°C (typically 20°C for 30 min) makes the surface hydrophilic and causes the cells to detach without the use of enzyme digestion reagent. When grafted PIPAAm layer thickness is between 15 and 20 nm, temperature-dependent cell adhesion and detachment can be observed. Once the cells spread and confluent on the surface, they can be spontaneously detached as a contiguous cell sheet by reducing the temperature. This process does not disrupt the cell-cell junctions because no enzymes like trypsin are required. Additionally, basal surface extracellular matrix (ECM) proteins such as fibronectin are preserved after detachment which enables easy attachment of cell sheets to host tissues and even wound sites with minimal cell loss. In order to obtain tissue constructs with characteristic physiological cellular functions *in vitro*, heterotypic cell-cell interactions are inevitable. As shown in Fig. 2, it is possible to modify the above-mentioned technique in order to develop patterned cell sheets using two or more kinds of cell source. Domains on petri dishes were grafted by using area-selective electron beam polymerization of PIPAAm. After cells were cultured on the patterned surfaces at 37°C , the temperature was decreased to 20°C . Cells on the PIPAAm surface are detached where other cell types were seeded subsequently by increasing the temperature to 37°C . Therefore, two cell types can be co-cultured in desired places which improve cellular functions [18, 38, 39]. Three-dimensional myocardial tubes

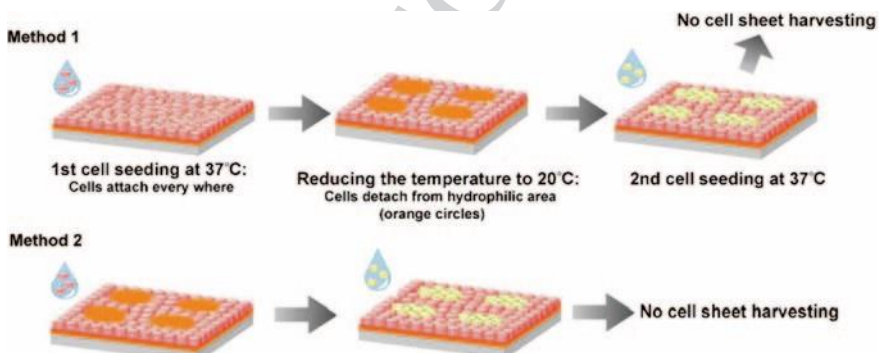


Fig. 2 Schematic diagram of methods of cell seeding for patterned co-culture on PIPAAm-grafted surfaces. (Adapted from[40])

159 were fabricated using neonatal rat cardiomyocyte sheets cultured on temperature 160 responsive culture dishes [40, 41]. Due to the functional gap junction formation, 161 electrical coupling of cardiomyocyte sheets was obtained quickly and the construct 162 was implanted [42]. Four weeks after the implantation, the myocardial tubes were 163 integrated with the host tissues showing spontaneous and synchronized pulsation 164 [38, 43]. Using this versatile method, functional and transplantable tissue sheets are 165 produced from different cell types including epidermal keratinocytes [44], kidney 166 epithelial cells [45] and periodontal ligaments [46, 47].

167 Two-dimensional cell patterning or cell-sheet based approaches have been suc-
168 cessful tissue engineering approaches. However, the engineered constructs
fabri169 cated with these methods are limited to 2D cell patterns or simple shapes
because 170 of the flat and uncontrolled shape of the cell sheets. In addition, many
sheets also 171 need to be culminated in high amount of cells which requires pre-
vascularization 172 of the sheets for 3D tissue constructs. Therefore, several
bioprinting approaches 173 have been developed for fabricating 3D tissue
constructs with live cells. Two major 174 approaches, ink-jet based and extrusion
based 3D bioprinting methods will be ex175 plained in details below.

176

177

178 **2.2 Inkjet-Based Bioprinting**

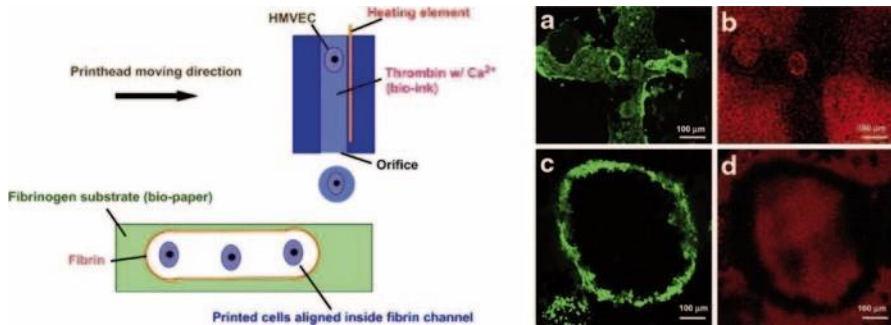
179

180 In inkjet-based bioprinting, a bioink made of cells and biomaterials are printed in 181 the form of droplets through cartridges onto a substrate. There are two types of 182 inkjet printing including continuous inkjet printing (CIJ) and drop-on-demand ink 183 jet printing (DOD). In CIJ mode, a jet is obtained by forcing the liquid through an 184 orifice under an external pressure and it breaks up into a stream of droplets. In DOD 185 mode, a pressure pulse is applied into the fluid which generates drops only when 186 needed. For ink-jet printing of cells, there are two most commonly used approaches: 187 thermal and piezo-electric inkjet printing. For thermal inkjet printing, small vol 188 umes of the printing fluid are vaporized by a micro-heater to create the pulse that 189 expels droplets from the print head. In piezoelectric inkjet printing, a direct me 190 chanical pulse is applied to the fluid in the nozzle by a piezoelectric actuator, which 191 causes a shock wave that forces the bioink through the nozzle [48]. However, there 192 have been only a few examples of cell deposition by piezoelectric ink-jet printing 193 due to the electrically conducting ink formulations and contamination concerns on 194 ink recycling [24].

195 Inkjet-based bioprinting (Fig. 3) enables to deposit different cell types in precise 196 orientations relative to the print surface and to each other at micrometer resolution 197 by

controlling the ejection nozzles and timing of spray [49]. Wilson and Boland first¹⁹⁸ adapted the ink-jet printers for the manufacture of cell and protein arrays, which¹⁹⁹ have the advantage of being fully automated and computer controlled [50]. In their²⁰⁰ next study, cell aggregates were printed onto thermosensitive gels layer-by-layer²⁰¹ in order to demonstrate the fusion between the closely-placed cell aggregates [51].

202 The same group deposited CHO cells and rat embryonic motoneurons as an ‘ink’



AQ1 Fig. 3 Schematic diagram of inkjet bioprinting methods of cells with fibrin channel scaffold printed microvasculature. **a** Printed perpendicular microvasculature cultured for 14 days. **b** Integrity of the printed structure stained using Texas Red conjugated dextran molecules of 3000 MW. **c** Printed ring shaped microvasculature cultured for 21 days. **d** Integrity of printed structure cultured for 21 days

203 onto several ‘bio-papers’ made from soy agar and collagen gel. They demonstrated
204 also that the mammalian cells can be effectively delivered by a modified thermal
205 inkjet printer onto biological substrates and that they retain their ability to function
206

[52]. Cui and Boland used also thermal inkjet printing to produce cell containing
207 fibrin channels by printing human microvascular endothelial cells onto thin layers
208 of fibrinogen as shown in Fig. 3. During the incubation period, the cells proliferated
209 and formed branched tubular structures mimicking simple vasculature [53].
210

Inkjet bioprinting has been progressed to fabricate 3D biological structures by
211 the use of readily crosslinked hydrogels such as alginate. In published studies, cells
212 have been mixed with alginate solutions and crosslinked with calcium chloride to
213 create cell encapsulating hydrogels having defined 3D structures [54–56]. In a more
214 recent study, alginate has been used as a constituent of bioink and it was mixed with
215

NIH 3T3 mouse fibroblasts cell suspension in order to fabricate zigzag cellular
216 tubes with an overhang structure using a platform-assisted 3D inkjet
bioprinting

217 system [57].

218

219 Although inkjet bioprinting has been one of the most commonly used method
220 in printing living cells and biomaterials, cell aggregation, sedimentation and cell-
221 damage because of the high shear stresses are common drawbacks of this method.

222

223 Cell aggregation and sedimentation may be prevented by frequent stirring of the
224 cell mixture, which can result in reduced cell viability if the cells are sensitive to the
225 shear forces [58]. Another problem limiting the inkjet bioprinting is the clogging
226 of the nozzle orifice. Low viscosity surfactants can be added to the ink which can
227 cause additional challenges such as cell damage [59].

228

229 Recently, two research groups successfully address the sedimentation and cell
230 aggregation problem during the inkjet bioprinting. Chahal and coworkers used a
231 surfactant (Ficoll PM400) create neutrally buoyant MCF-7 breast cancer cell sus-
232 pensions, which were ejected using a piezoelectric drop-on-demand inkjet printing

233

234 system. They demonstrated that Ficoll PM400 did not have adverse effects on cell
235 viability. Moreover, neutrally buoyant suspension greatly increased the reproducibility
236 of consistent cell counts, and eliminated nozzle clogging. [60].

237 Ferris et al. used two different commercially available drop-on-demand printing
238 systems in order to reproducibly print several different cell types over long printing
239 periods. The bio-ink based on a novel microgel suspension in a surfactant-containing
240 tissue culture medium can prevent the settling and aggregation of cells, while
241 meeting the stringent fluid property requirements needed for many-nozzle commercial
242 inkjet print heads. They could print two cells types simultaneously from two
243 different inkjet print heads, which is a innovative way to biofabricate more complex
244 multi-cellular structures [61].

245

246

243 **2.3 Self-Assembly Based Bioprinting**

244

245 The autonomous organization of components from an initial state into a final pattern
246 or structure without external intervention is called self-assembly. The aim of the

247 self-assembly-based bioprinting is the use of the inherent organizational capacity of
248 cells into tissues and eventually organs by mimicking natural morphogenesis. The

249 best examples of tissue self-organization and self-assembly are in the field of devel-
250 opmental biology and scaffold-free biomimetic approach has deep roots in devel-
251 opmental biology [20]. Malcolm Steinberg published papers, in which he
252 formulated fundamental thermodynamic rules determining tissue self-assembly
and developed

²⁵³ differential adhesion hypothesis (DAH) explaining the fluidic nature of cell sorting ²⁵⁴ and tissue self-assembly [62–64]. Therefore, the novel scaffold-free biomimetic tis²⁵⁵ sue engineering paradigm relies on the principle that in vitro tissue assembly from ²⁵⁶ single cells or tissue aggregates is feasible.

²⁵⁷ Based on the self-assembly principle, it is possible to fabricate reliable and re²⁵⁸ producible 3D tissue constructs having defined topology and functionality in vitro ²⁵⁹ when combined with bioprinting techniques. The disadvantage of this method is

²⁶⁰ that the development of the natural ECM is time consuming and in vitro self-as²⁶¹ sembly may vary with fully physiological conditions. The bioprinting of 3D tissue

²⁶² constructs is achieved via a three-phase process: (1) preprocessing or bio-ink prepa²⁶³ ration; (2) processing, i.e. the actual automated deliver/printing of the bio-ink parti²⁶⁴ cles into the bio-paper by the bioprinter; and (3) postprocessing, i.e. the maturation/

²⁶⁵ incubation of the printed construct in the bioreactor [19]. Self-assembly occurs in an ²⁶⁶ *in vivo* like, fully controllable cell environment (bioreactor) by the differentiation of ²⁶⁷ cells at the right time, in the right place and into the right phenotype and eventually ²⁶⁸ the assembly of them to form functional tissues. Based on this approach, a perfusion ²⁶⁹ reactor is used for the maturation of a bioprinted macrovascular network in order

²⁷⁰ to obtain the required mechanical properties. Microvascular units consisting of cy²⁷¹ lindrical or spherical multicellular aggregates were fabricated by the parenchymal ²⁷² and endothelial cells. Afterwards, microvascular units were located in the macro²⁷³ vascular network for the perfusion supporting self-assembly and the connection to

²⁷⁴ the existing network. Multicellular spherical and cylindrical aggregates have been

²⁷⁵

²⁷⁶

²⁷⁷

²⁷⁸

²⁷⁹

²⁸⁰

²⁸¹

²⁸²

²⁸³

²⁸⁴

²⁸⁵

²⁸⁶

²⁸⁷

²⁸⁸

²⁸⁹

²⁹⁰

²⁹¹

²⁹²

constructed by using 3D printing methods, which enable to achieve flexibility in tube diameter and wall thickness and to form branched tubular structures. However, the printed cell aggregates should be perfectly supported by hydrogels for 3D printing [21]. Forgacs and his group employed this novel technology to print cellular topologically defined structures of various shapes. Cardiac constructs were built using embryonic cardiac and endothelial cells and their postprinting self-assembly resulted in synchronously beating solid tissue blocks, where the endothelial cells were organized into vessel-like conduits [65]. In their more recent study, the same group utilized the self-assembly approach in order to bioprint small-diameter, multi-layered, tubular vascular and nerve grafts using bio-ink composed of aortic smooth muscle cells (HASMC), human aortic endothelial cells (HAEC), human dermal fibroblasts (HDFb) and bone marrow stem cells (BMSC), respectively as shown in Fig. 4 [25]. Similarly, in another study, self-assembled cell-based microtissue blocks were used to generate small diameter tissue-engineered living blood vessels (TEBV). Microtissues composed of human-artery-derived fibroblasts (HAFs) and endothelial cells (HUVECs) were cultured for 7 and 14 day under pulsatile flow/mechanical stimulation in a designed bioreactor or static culture conditions with a diameter of 3 mm and a wall thickness of 1 mm. Self-assembled microtissues

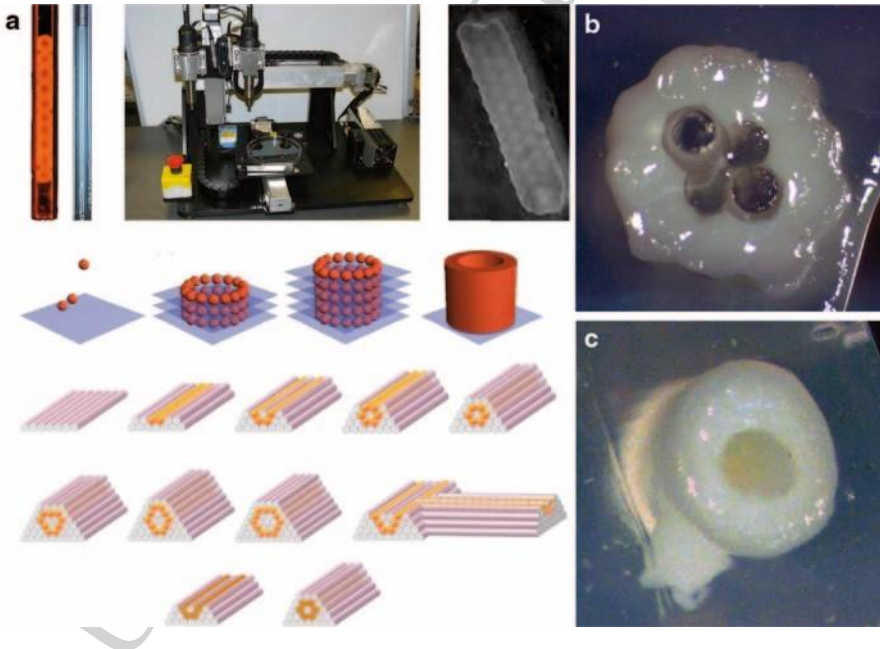


Fig. 4 **a** Organovo bioprinter with cell and hydrogel printing heads and schematics to print tubular structures with cellular spheroids: layer-by-layer deposition of spheroids into the hydrogel. **b** Cross-section of a vascular graft printed with four central rods 12 h post-printing. All cellular cylinders have fused to form a continuous conduit. **c** A vascular construct (ID =600 μm) at 14 days post-perfusion. (Adapted from [25])



Fig. 5 Bioprinting of aortic valve conduit. **a** Aortic valve model reconstructed from micro-CT images. The root and leaflet regions were identified with intensity thresholds and rendered separately into 3D geometries into STL format (*green* color indicates valve root and *red* color indicates valve leaflets); **b**, **c** schematic illustration of the bioprinting process with dual cell types and dual syringes; **b** root region of first layer generated by hydrogel with SMC; **c** leaflet region of first layer generated by hydrogel with VIC; **d** fluorescent image of first printed two layers of aortic valve conduit; SMC for valve root were labeled by cell tracker *green* and VIC for valve leaflet were labeled by cell tracker *red*. **e** as-printed aortic valve conduit. (Reproduced with permission [75]).

293 composed of fibroblasts showed accelerated ECM formation and a layered tissue **AQ2**
 formation was obtained only in flow/mechanical stimulation conditions [66] Fig. 5. ■

295 An alternative approach for multicellular spheroid assembly technique for bio296
 fabrication was developed by Nakayama and his group. In their technique, they 297 used a so
 called needle-array system instead of using a bioprinter. A robotic system 298 was developed
 in order to skewer the multicellular spheroids into medical-grade
 299 stainless needles, which served as temporal fixators until multicellular spheroids 300 fused
 each other. They could fabricate complex 3D scaffold-free cell constructs 301 with different
 types of cells including chondrocyte, hepatocyte, cardiomyocyte and 302 vascular smooth
 muscle cell. One of the advantages of this technique is the easy 303 removal of the temporary
 supports without contamination with exogenous materi-
 304 als [3].

305 Apart from the above mentioned applications, a new method is presented to rap306
 idly self-assemble cells into 3D tissue rings without the use of additional equip307
 ment. This method enables fabrication of engineered tissue constructs entirely from
 308 cells by seeding cells into custom made annular agarose wells with 2, 4 or 6 mm
 309 inside diameters. Different cell types including rat aortic smooth muscle cells
 and

310 human smooth muscle cells are used with varying seeding conditions and culture
 length to form tissue rings. The strength and modulus of tissue rings increased with
 311 ring size and decreased with culture duration. Rat smooth muscle cell rings with
 an 312 inner diameter of 2 mm are cohesive enough for handling after 8 days
 incubation 313 and they yield at 169 kPa ultimate tensile strength. Furthermore, it
 is also pos314 sible to fabricate tissue tubes by transferring the rings onto silicone
 tubes, sliding 315 them into contact with one another and incubating them for an
 additional 7 days. 316 Although these rings are not as strong as ring segments of
 native blood vessels or 317 TEBV fabricated from cell sheets for 2–3 months, the
 presented method allows de318 veloping 3D tissue constructs from aggregated cells
 within an experimentally useful ³¹⁹ time frame (1–2 weeks) [67]. Likewise created
 smooth muscle cell tissue rings and 320 rings fabricated from cells seeded in fibrin
 or collagen gels are compared based on 321 their relative strength and utility for
 tissue engineering. All tissue rings were cul322 tured for 7 days in supplemented
 growth medium which includes ϵ -amino caproic

323 acid, ascorbic acid, and insulin-transferrin-selenium. Ultimate tensile strength and 324
 stiffness values of tissue rings were two-fold higher than fibrin gel and collagen gel 325

rings. Tissue rings cultured in supplemented growth medium exhibit a three-fold increase in tensile strength and stiffness in comparison to the tissue rings cultured in standard growth medium [68].

The approach of using microtissues as building blocks to form larger structures is further used by other research groups in order to investigate the capacity of cell aggregates. After a preculture period for 7 days of HUVEC spheroids, they were mixed with NHF cells and were able to reassemble and form microtissues

with the NHF cells on the inside and coated with HUVEC on the outside [69]. Additionally, the kinetics of the cellular self-assembly also differs from one cell type to the other. While H35 cells formed relatively stable rod structures inside the recesses of micromolded agarose gels, NHF cells reassembled quickly the initial rod structures to a final spheroid structure [70].

337

338

339 **2.4 Extrusion-Based Bioprinting**

340

341

Bioprinting methods based on extrusion of cell or cell-laden biomaterials use self-assembly cells to construct 3D biological constructs. The main principle of extrusion-based bioprinting techniques is to force continuous filaments of materials including hydrogels, biocompatible copolymers and living cells through a nozzle with a help of a computer to construct a 3D structure [27]. Extrusion-based printers usually have a temperature-controlled material handling and dispensing system and stage with the movement capability along the x, y and z axes. The printers are directed by the CAD-CAM software and continuous filaments are deposited in two dimensions layer-by-layer to form 3D tissue constructs. The stage or the extrusion head is moved along the z axis, and the printed layers serve as a base and support for the next layer. Pneumatic or mechanical (piston or screw) are the most common techniques to print biological materials for 3D bioprinting applications [33]. Additionally, novel multi-nozzle biopolymer deposition systems were developed for freeform fabrication of biopolymer-based tissue scaffolds and cell-embedded tissue

constructs [71, 72].

357 An extrusion-based printer was used to deposit living cells by Williams and co-workers.

358 Instead of using a thermally crosslinked biomaterial, which can flow

359 at room temperature, but crosslink into a stable material at body temperature, they used Pluronic F-127 and type I collagen to encapsulate human fibroblasts and bovine aortic endothelial cells (BAECs) separately. These materials flow at physiologically suitable temperatures (35–40°), but crosslink at room temperature. They demonstrated the availability of CAD/CAM technology to fabricate anatomically correct shaped constructs and also examined several environmental factors with respect to the viability of the extruded cells [73, 74]. Recently, different research groups used the similar extrusion systems in order to fabricate anatomically accurate and mechanically heterogeneous aortic valves as shown in Fig. 1 [75, 76].

369 Several groups used high resolution extrusion systems to print different type of cells encapsulated in various hydrogels. For instance, Chang et al. printed HepG2

cell encapsulated sodium alginate through a pneumatically powered nozzle and examined the process parameters, the dispensing pressure and the nozzle diameter, regarding the cell viability and recovery [77]. In another study, alginate hydrogel was used with calcium sulfate as a crosslinking agent to fabricate pre-seeded plants of arbitrary geometries and the printed constructs showed high viabilities [78]. Although the cell viability after printing is important, it is also important that the cells perform their essential functions in the tissue constructs.

Extrusion-based printing allows the construction of organized structures within a realistic time frame, and hence it is the most promising bioprinting technology.

The main advantage of extrusion-based bioprinting is the ability to print very high cell densities. Some groups developed 3D bioprinters in order to use multicellular spheroids or cylinders as bioink to create 3D tissue constructs [19, 21, 25, 79–81]. However, preparing bioink requires time-consuming manual operation and makes totally automated and computer-controlled 3D bioprinting impossible in earlier

studies. Therefore, our group focused on the development of a continuous printing approach in order to extrude cylindrical multicellular aggregates using an extrusion-based bioprinter, which is an automated, flexible platform designed to fabricate 3D tissue engineered cell constructs. In order to bioprint anatomically correct tissue constructs directly from medical images, the targeted tissue or organ must be biomodeled. In the following section, the details of modeling and developing path planning for automated direct cell bioprinting will be explained.

392

393

2.4.1 Biomodeling

394

395

In order to obtain an anatomically accurate tissue constructs, several imaging methods for data acquisition of tissue organ such computed tomography (CT) and magnetic resonance imaging (MRI) could be used. The obtained medical images are then transferred to a special segmentation software, where the images are represented with stack of numerous planar scan captures (Fig. 6a). The segmented 3D

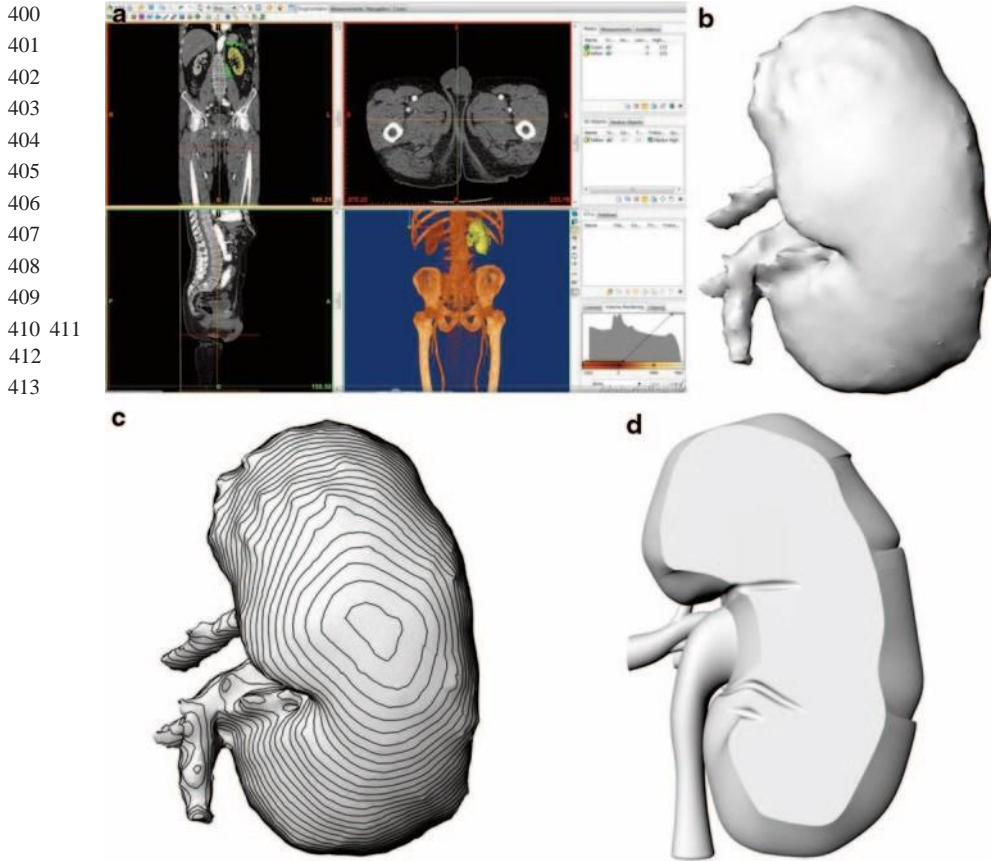


Fig. 6 Biomodeling of the bioprinted tissue/organ **a** segmentation of the targeted tissue/organ **b** mesh model of segmented model **c** slicing of CAD model

surface geometry is transformed to a CAD model which is a mesh model of the object (Fig. 6b). In order to generate bioprinting path planning as well as the topology optimization for bioprinting processes, the resultant mesh models need to be represented by smooth parametric surfaces. The mesh model is then sliced with consecutive planar cross-sections, resulting in closed contour curves for each thin layer slice [28] (Fig. 6c). Those contour curves are basically the surface boundaries of tissue constructs. Obtained contour curves need to smoothed by B-spline curve fitting from their control points, in order to generate smooth parametric surfaces and finer surface geometry (Fig. 6d). The resultant CAD model is then ready to be used for path planning and topology optimization purposes for biomimetic 3D bioprinting.

Recently, novel computer-aided algorithms and strategies are developed to model and 3D bioprint a scaffold-free human aortic tissue construct biomimetically by our group. Medical images obtained from magnetic resonance imaging (MRI) are used



Fig. 7 Biomimetic modeling of aorta directly from medical images **a** segmentation from medical images **b** Conversion to a CAD model

414 to obtain the geometric and topological information of the targeted aorta. In order to 415
 obtain 3D computer models of the aortic tissue, MRI images are segmented using a 416
 segmentation software and converted into CAD model (Fig. 7). For tool path plan⁴¹⁷ ning as
 well as for optimization of 3D bioprinting, the resultant mesh model of aorta⁴¹⁸ converted
 to a CAD model with smooth parametric surfaces. Three-dimensional⁴¹⁹ bioprinting path
 planning and parameter optimization are then developed. The de⁴²⁰ veloped self-supporting
 methodology is used to calculate corresponding tool paths⁴²¹ for both cell aggregates and
 the support structures, which control the bioprinter for⁴²² 3D printing of a biomimetic aortic
 construct [74].

423
 424

425 **2.4.2 Path Planning and Optimization for Bioprinting** 426

427 In order to bioprint an anatomically correct tissue constructs with live cells layer-by⁴²⁸
 layer, the generated computer model of this construct needs to be sliced by planar
 429 cross-sections, resulting in closed contour curves for each layer. Then those layers⁴³⁰
 need to be filled by appropriate types of cellular aggregates with supportive hydro⁴³¹ gel
 walls surrounding them for keeping the biomimetic form. In our recent work,⁴³²
 multicellular cell aggregates are 3D bioprinted based on computer-aided continuous⁴³³ and,
 interconnected tool-path planning methodologies. Continuous bioprinting en⁴³⁴ ables to
 design and 3D bioprint extruded multicellular aggregates according to the
 435 computer model of the targeted tissue. The Zig-zag and Contour Offsetting pattern⁴³⁶
 tool-path methodologies are developed to 3D bioprint different shaped structures⁴³⁷ with
 multiple layers. A CAD software package was used for developing algorithms⁴³⁸ for
 continuous and connected bioprinting path plans. In order to keep the 3D forms⁴³⁹ of printed
 structures during the maturation period, a biocompatible and bio-inert
 440 agarose-based hydrogel was used as a support material [75]. The developed bio⁴⁴¹
 printing process starts from the bottom layer and follows the generated path plan for⁴⁴² each
 particular layer consecutively through the top layer. At a layer, support mate⁴⁴³ rial enclosing
 the cellular aggregates are printed first, and then cellular aggregates⁴⁴⁴ are deposited to fill
 the respective contour areas.

445 In Fig. 8, schematic view of pat planning strategies are showed for a layer. Figure
 8a-b shows Zig-zag whereas Fig. 8c-d shows Contour Offsetting path planning.

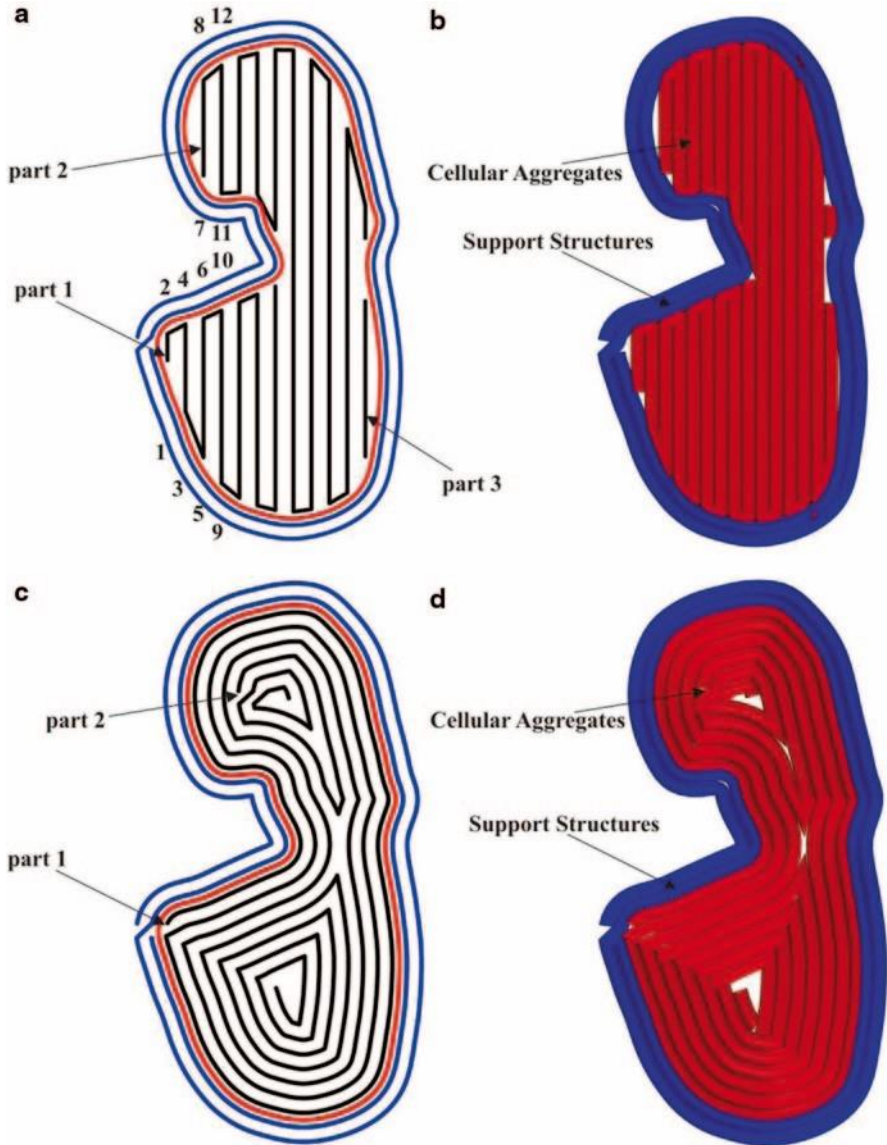


Fig. 8 Path planning for bioprinting **a–b** Zig-zag pattern **c–d** Contour offsetting path planning

In both Zig-zag and Contour Offsetting patterns, outer supportive hydrogel walls' 447 tool path are generated with offsetting the contour curve with a deposited cellular 448 or hydrogel extrusion diameter. Placement of support structures before the cellular 449 aggregates provides necessary conditions for cell fusion and structure conservation. 450 In Zig-zag pattern path planning strategy, contour curves are

crossed with parallel consecutive lines, each separated by extrusion diameter, and an intersection point is generated for each cross as shown in Fig. 8a. Zig-zag pattern path planning strategy aims to fill the contour area by following a zig-zag patterned path way between the generated intersection points as uninterrupted as possible.

In Contour Offsetting path plan strategy, cellular aggregates' path plan is formed by offsetting the contour curve to fill the entire area. After the necessary amount of offset curves is generated, they are joined by small line segments to enable continuous bioprinting. That strategy also aims to fill the contour area with minimum number of cellular aggregate as shown in Fig. 8c).

After the path plan is calculated, the coordinates of these movements are transferred to bioprinter to guide the deposition path plan in order to obtain anatomically correct tissue constructs. In Fig. 8b and Fig. 8d, the finalized generated path plans of cellular aggregates (red) and support structures (blue) are shown for both path planning strategies.

465

466

467 **2.4.3 Continuous Cell Printing**

468

In our recent work, a novel bioprinting method is used for precise deposition of multicellular aggregates composed of different combinations of mouse aortic smooth muscle cells (MOVAS), NIH 3T3 mouse fibroblast cells, human umbilical vein endothelial cells (HUVEC), and human dermal fibroblast (HDF) cells according to computer-generated paths as shown in Fig. 9 [83]. The proposed methodology increases the contact of cylindrical multicellular aggregates in adjacent bioprinted layers, facilitates the fusion of cells and accelerates the maturation process. More significantly, this procedure reduces the human intervention at forming of cylindrical multicellular aggregates and therefore, increases the reproducibility.

The printed 3D multicellular structures are examined for their mechanical strength, shape deformation with time, cell viability and cell fusion. The printed constructs having different shapes deformed during the incubation period (up to

10-days) and generally a shrinking between 20 – 38 % was observed. After 4 or 7 days incubation, the support structures of well-defined and random-shaped printed structures composed of MOVAS, HUVEC and NIH 3T3 multicellular aggregates were manually removed and the fused cell structures could be transferred with forceps into a falcon filled with PBS (Fig. 10a). It is remarkable that the stripe shaped constructs composed of HUVEC/HDF cell aggregates had a small deformation percentage (85 % after 3-days incubation) and were sufficiently sturdy to be handled and transferred as shown in Fig. 10b.[83]. MOVAS/HUVEC/NIH 3T3 multicellular aggregates fused within 3 days, which corresponds to earlier studies [25, 81]. The cell viability upon implementation was high (97 %) showing that the cellular bioink preparation method is successful in comparison to other studies in literature. It

seems that multicellular aggregates composed of human cells have better mechanical properties.

493
494
495
496
497
498
499
500
501
502
503
504
505
506

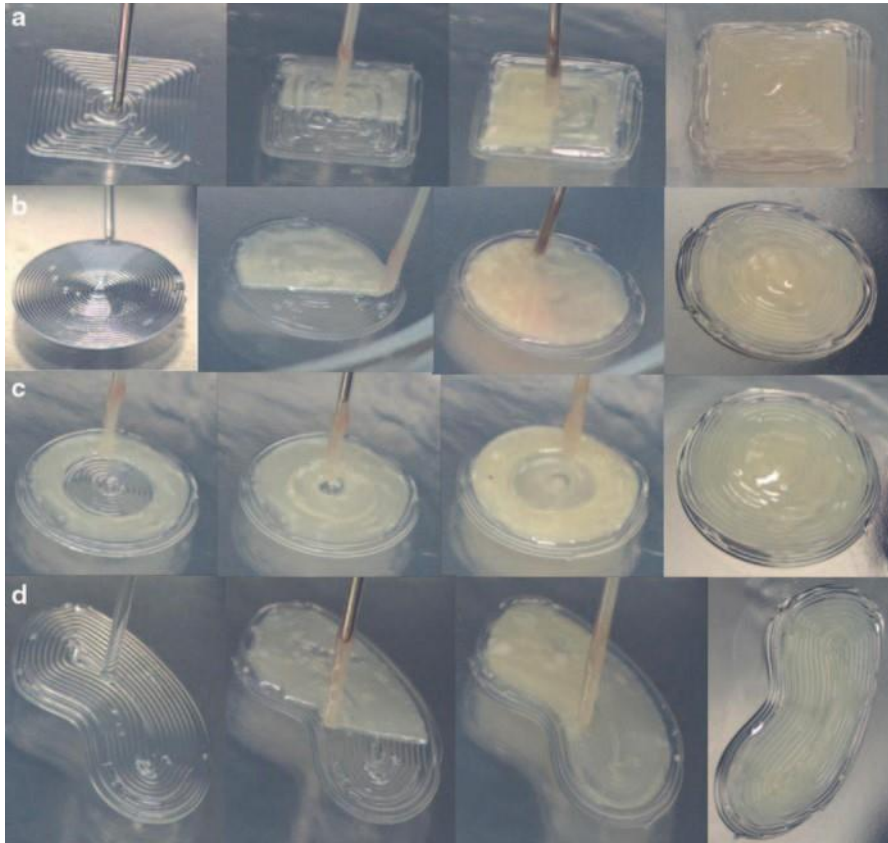


Fig. 9 Continuous bioprinting of live cells directly from computer models **a** *Rectangular* shaped **b** *Random-shaped* **c** *Zig-zag patterned circular* **d** *Spiral patterned circular* printed structures [83]

3 Conclusion and Discussion on Stem Cell Printing

Bioprinting is one of the most promising techniques in tissue engineering, where living cells are deposited layer-by-layer with or without biomaterials in user-defined patterns to build 3D tissue constructs. However, there are some challenges related with technical, material and cellular aspects. 3D bioprinting technology requires increased resolution, speed and compatibility with biologically relevant materials. Especially, the fabrication speed must be increased to create structures of clinically relevant sizes. Even the cells used for bioprinting applications are robust enough to survive the bioprinting process and withstand the physiological stresses; a large cell construct in an open environment may not survive a slow and therefore long printing process. For bioprinting, well-characterized and reproducible source of cells is required and any cell type selected for printing should be able to be proliferated into sufficient numbers for printing. Additionally, the proliferation

507 508
 509
 510 511
 512
 513
 514
 515
 516
 517
 518
 519
 520
 521
 522
 523
 524
 525

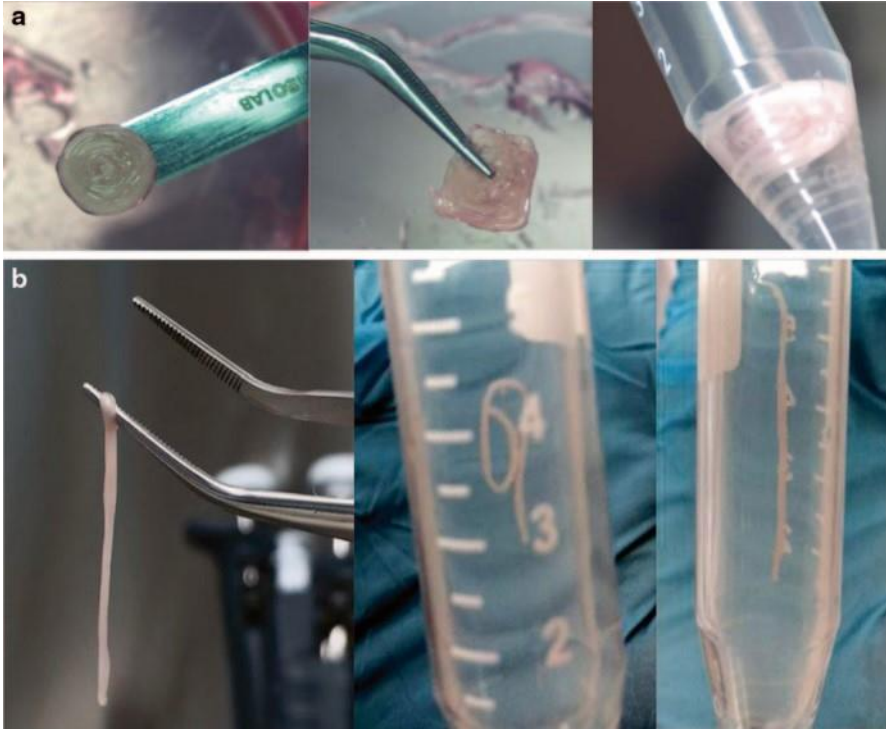


Fig. 10 Bioprinted 3D totally biological tissue constructs without any biomaterial. **a** Circular and square shaped bioprinted with MOVAS, HUVEC and NIH 3T3 multicellular aggregates. **b** Stripe shaped bioprinted with HUVEC/HDF cell aggregates [83]

rate and the differentiation with small molecules or other factors should be controllable. Furthermore, sufficient vascularization and capillaries/microvessels are required for long-term viability of the fabricated construct and for tissue perfusion, respectively. The engineered structure should have suitable mechanical properties for physiological pressures and for surgical connection in case of transplantation. Bioreactors are used to maintain tissues *in vitro* and to provide maturation factors as well as physiological stressors for assembly, differentiation and ECM production prior to *in vivo* implantation.

Stem cells such as mesenchymal, induced pluripotent and embryonic stem cells could be a great source for bioprinting. Especially, printing differentiated or progenitor cells precisely and spatially could lead to multi-functional tissue constructs or even organs. However several challenges need to be overcome. First, bioprinting with stem cells requires large number of cells. Culturing this amount of stem cells could be really difficult. Especially, growing large number of stem cells on a feeder layer or special growth medium is really challenging. Even after culturing enough number of stem cells, bioprinting stem cells precisely and spatially accurate manner would require highly precise and special bioprinters. During bioprinting, the effect of compression on the viability and differentiation of stem cells should be considered. Since the stem cells are more susceptible to bioprinting conditions, more gentle and short printing procedures should be developed. Although the current 3D

528 bioprinting technology shows a great deal of promise to generate 3D layered constructs using live mixed cell populations, there is still a long way to go to create a fully-functional organ.

531
532
533

References

534

- 536 1. Langer R, Vacanti JP. Tissue engineering. *Science*. 1993;260(0036-8075 (Print)):920–6.
- 537 2. Pollok JM, Vacanti JP. Tissue engineering. *Semin Pediatr Surg*. 1996;8:586(1055-8586 (Print)):191–6.

AQ3 38 3. Nakayama K. In vitro biofabrication of tissues and organs. In: Forgacs G, Sun W, editors. *Biofabrication: micro- and nano-fabrication, printing, patterning and assemblies*. Elsevier;

- 540 2013. p. 1–16.
- 541 4. Atala A, Bauer SB, Soker S, Yoo JJ, Retik AB. Tissue-engineered autologous bladders for 542 patients needing cystoplasty. *Lancet*. 2006;367(9518):1241–6.
- 543 5. Brittberg M, Nilsson A, Lindahl A, Ohlsson C, Peterson L. Rabbit articular cartilage defects 43 treated with autologous cultured chondrocytes. *Clin Orthop Relat Res*. 1996;326(0009-921X

- 544 (Print)):270–83.
- 545 6. Gallico GG, O'Connor NE, Compton CC, Kehinde O, Green H. Permanent coverage of large 546 burn wounds with autologous cultured human epithelium. *New Engl J Med*. 1984;311(7):448–

- 547 51.
- 548 7. Hibino N, McGillicuddy E, Matsumura G, Ichihara Y, Naito Y, Breuer C, et al. Late- 549 term results of tissue-engineered vascular grafts in humans. *J Thorac Cardiovasc Surg*. 2010;139(2):431–6.e2.

- 550 8. Matsumura G, Ishihara Y, Miyagawa-Tomita S, Ikada Y, Matsuda S, Kurosawa H, 551 Shin'oka T, et al. Evaluation of tissue-engineered vascular autografts. *Tissue Eng*. 2006;12(1076-3279 (Print)):3075–83.

- 552 9. Niemeyer P, Krause U, Fellenberg J, Kasten P, Seckinger A, Ho AD, Simank HG, et al. Eval 553 uation of mineralized collagen and alpha-tricalcium phosphate as scaffolds for tissue 554 neering of bone using human mesenchymal stem cells. *Cells Tissues Organs*. 2004;177(2) 555 (1422-6405 (Print)):880–5.

- 556 10. Oberpenning F, Meng J, Yoo JJ, Atala A. De novo reconstitution of a functional mammalian 557 urinary bladder by tissue engineering. *Nat Biotech*. 1999;17(2):149–55.

- 558 11. Radisic M, Park H, Shing H, Consi T, Schoen FJ, Langer R, et al. Functional assembly of 558 engineered myocardium by electrical stimulation of cardiac myocytes cultured on scaffolds.

- 559 *Proc Nati Acad Sci*. 2004;101(52):18129–34.

- 560 12. Shin'oka T, Matsumura G, Hibino N, Naito Y, Watanabe M, Konuma T, et al. Midterm 561 cal result of tissue-engineered vascular autografts seeded with autologous bone 562 marrow cells. *J Thorac Cardiovasc Surg*. 2005;129(6):1330–8.

- 563 13. Nakamura M, Iwanaga S, Henmi C, Arai K, Nishiyama Y. Biomatrices and biomaterials for 563 future developments of bioprinting and biofabrication. *Biofabrication*. 2010;2(1):014110. 564 14. Wüst S, Müller R, Hofmann S. Controlled positioning of cells in biomaterials—approaches 565 towards 3D tissue 566 printing. *J Funct Biomater*. 2011;2(3):119–54.

- 566 15. Melchels FPW, Domingos MAN, Klein TJ, Malda J, Bartolo PJ, Huttmacher DW. Additive 567 manufacturing of tissues and organs. *Prog Polym Sci*. 2012;37(8):1079–104.

- 568 16. Khoda AKM, Ozbolat IT, Koc B. A functionally gradient variational porosity architecture for

- 568 hollowed scaffolds fabrication. *Biofabrication*. 2011;3(3):034106.
569
- 570 17. Khoda AKM, Ozbolat IT, Koc B. Designing heterogeneous porous tissue scaffolds for additive
571 manufacturing processes. *Comput-Aided Des*. 2013;45(12):1507–23.
- 572 18. Matsuda N, Shimizu T, Yamato M, Okano T. Tissue engineering based on cell sheet technol-
573 ogy. *Adv Mater*. 2007;19(20):3089–99.
- 574 19. Mironov V, Prestwich G, Forgacs G.
575 Bioprinting living structures. *J Mater Chem*. 2007;17(20):2054–60.
- 576 20. Mironov V, Visconti RP, Kasyanov V, Forgacs G, Drake CJ, Markwald RR. Organ printing: 576
577 tissue spheroids as building blocks. *Biomaterials*. 2009;30(12):2164–74.
- 578 21. Jakab K, Norotte C, Marga F, Murphy K, Vunjak-Novakovic G, Gabor F. Tissue engineering
579 by self-assembly and bio-printing of living cells. *Biofabrication*. 2010;2(2):022001. 578
- 580 22. L'Heureux N, Dusserre N, Konig G, Victor B, Keire P, Wight TN, et al. Human tissue-engineered
581 neered blood vessels for adult arterial revascularization. *Nat Med*. 2006;12(3):361–5.
- 582 23. L'Heureux N, Pâquet S, Labbé R, Germain L, Auger FA. A completely biological tissue-engineered
583 human blood vessel. *FASEB J*. 1998;12(1):47–56.
- 584 24. Ferris C, Gilmore K, Wallace G, in het Panhuis M. *Biofabrication: an overview of the ap*
585 586 587 588 589 590
591 592 593 594 595 596 597 598 599 600 601 602
592 approaches used for printing of living cells. *Appl Microbiol Biotechnol*. 2013;97(10):4243–58. 583 25. Marga
584 F, Jakab K, Khatiwala C, Shepherd B, Dorfman S, Hubbard B, et al. Toward engineer-
585 ing functional organ modules by additive manufacturing. *Biofabrication*. 2012;4(2):022001.
- 586 26. Forgacs G, Foty RA, Shafir Y, Steinberg MS. Viscoelastic properties of living embryonic tissues:
587 a quantitative study. *Biophys J*. 1998;74(5):2227–34.
- 588 27. Koç B, Hafezi F, Ozler SB, Kucukgul C. Bioprinting-application of additive manufacturing
589 in medicine. In: Bandyopadhyay A, Bose S, editors. *Additive manufacturing*. CRC Press; in
590 press.
- 591 28. Song S-J, Choi J, Park Y-D, Lee J-J, Hong SY, Sun K. A three-dimensional bioprinting sys-
592 tem for use with a hydrogel-based biomaterial and printing parameter characterization. *Artif*
593 *Organs*. 2010;34(11):1044–8.
- 594 29. Chang CC, Boland ED, Williams SK, Hoying JB. Direct-write bioprinting three-dimensional
595 biohybrid systems for future regenerative therapies. *J Biomed Mater Res B Appl Biomater*.
596 2011;98B(1):160–70.
- 597 30. Odde DJ, Renn MJ. Laser-guided direct writing for applications in biotechnology. *Trends*
598 *Biotechnol*. 1999;17(10):385–9.
- 599 31. Nahmias Y, Schwartz RE, Verfaillie CM, Odde DJ. Laser-guided direct writing for three-
600 dimensional tissue engineering. *Biotechnol Bioeng*. 2005;92(2):129–36.
- 601 32. Zhen M, Russell KP, Qin W, Julie XY, Xiaocong Y, Peng X, et al. Laser-guidance-based
602 cell deposition microscope for heterotypic single-cell micropatterning. *Biofabrication*.
2011;3(3):034107.
33. Murphy SV, Atala A. 3D bioprinting of tissues and organs. *Nat Biotech*. 2014;32(8):773–
85.
34. Guillotin B, Souquet A, Catros S, Duocastella M, Pippenger B, Bellance S, et al. Laser as-
sisted bioprinting of engineered tissue with high cell density and microscale organization.
Biomaterials. 2010;31(28):7250–6.

- 603 35. Barron JA, Ringeisen BR, Kim H, Spargo BJ, Chrisey DB. Application of laser printing to 604 mammalian cells. *Thin Solid Films*. 2004;453–454(0):383–7.
- 605 36. Ringeisen BR, Kim H, Barron JA, Krizman DB, Chrisey DB, Jackman S, Auyeung RY, et al. Laser printing of pluripotent embryonal carcinoma cells. *Tissue Eng*. 2004;(1076–3279
606 (Print))10(3–4):483–91.
- 607 37. Guillemot F, Souquet A, Catros S, Guillotin B, Lopez J, Faucon M, et al. High-throughput
la608 ser printing of cells and biomaterials for tissue engineering. *Acta Biomater*. 2010;6(7):2494–
609 500.
- 610 38. Haraguchi Y, Shimizu T, Yamato M, Okano T. Regenerative therapies using cell sheet-based tissue engineering for cardiac disease. *Cardiol Res Pract*. 2011;2011:845170.
- 611 39. Shimizu T, Yamato M, Isoi Y, Akutsu T, Setomaru T, Abe K, Kikuchi A, et al. Fabrication
612 of pulsatile cardiac tissue grafts using a novel 3-dimensional cell sheet manipulation tech-
613 nique and temperature-responsive cell culture surfaces. *Circul Res*. 2002;90(1524–4571
(Electronic)):e40.
- 614 40. Imen Elloumi H, Masayuki Y, Teruo O. Cell sheet technology and cell patterning for
615 biofab614 rication. *Biofabrication*. 2009;1(2):022002.
- 616 41. Shimizu T, Yamato M, Akutsu T, Shibata T, Isoi Y, Kikuchi A, et al. Electrically communi616 cating
three-dimensional cardiac tissue mimic fabricated by layered cultured cardiomyocyte 617 sheets. *J Biomed
Mater Res*. 2002;60(1):110–7.
- 618 42. Haraguchi Y, Shimizu T, Yamato M, Kikuchi A, Okano T. Electrical coupling of cardio-
619 myocyte sheets occurs rapidly via functional gap junction formation. *Biomaterials*.
2006;27(27):4765–74.
- 620 43. Shimizu T, Sekine H, Isoi Y, Yamato M, Kikuchi A, Okano T. Long-term survival and
621 growth
of pulsatile myocardial tissue grafts engineered by the layering of cardiomyocyte sheets.
Tis622 sue Eng. 2006;12(1076–3279 (Print)):499–507.
- 623 44. Yamato M, Utsumi M, Kushida A, Konno C, Kikuchi A, Okano T.. Thermo-responsive cul-
624 ture dishes allow the intact harvest of multilayered keratinocyte sheets without dispase by 624
reducing temperature. *Tissue Eng*. 2001;7(1076–3279 (Print)):473–80.
- 625 45. Kushida A, Yamato M, Isoi Y, Kikuchi A, Okano T. A noninvasive transfer system for polar626 ized
renal tubule epithelial cell sheets using temperature-responsive culture dishes. *Eur Cell 627 Materl*
2005;10(1473–2262 (Electronic)):23–30.
- 628 46. Akizuki T, Oda S, Komaki M, Tsuchioka H, Kawakatsu N, Kikuchi A, et al. Application of
629 periodontal ligament cell sheet for periodontal regeneration: a pilot study in beagle dogs. *J
Periodontal Res*. 2005;40(3):245–51.
- 630 47. Hasegawa M, Yamato M, Kikuchi A, Okano T, Ishikawa I. Human periodontal
631 ligament 631 cell sheets can regenerate periodontal ligament tissue in an athymic
rat model. *Tissue Eng*. 632 2005;11(1076–3279 (Print)):469–78.
- 633 48. Malda J, Visser J, Melchels FP, Jüngst T, Hennink WE, Dhert WJA, et al. 25th anniversary
634 article: engineering hydrogels for biofabrication. *Adv Mater*. 2013;25(36):5011–28.
- 635 49. Nakamura M, Kobayashi A, Takagi F, Watanabe A, Hiruma Y, Ohuchi K, Iwasaki Y, et al.
Biocompatible inkjet printing technique for designed seeding of individual living cells. *Tis636 sue
Eng*. 2005;11(1076–3279 (Print)):1658–66.

- 637 50. Wilson WC, Boland T. Cell and organ printing 1: protein and cell printers. *Anat Rec A: Discov Mol, Cell, Evol Biol.* 2003;272 A(2):491–6.
- 638
51. Boland T, Mironov V, Gutowska A, Roth EA, Markwald RR. Cell and organ printing 2: fu639 sion of cell aggregates in three-dimensional gels. *Anatomical Rec A: Discov Mol, Cell, Evol Biol.* 2003;272 A(2):497–502.
- 641 52. Xu T, Jin J, Gregory C, Hickman JJ, Boland T. Inkjet printing of viable mammalian cells. *Biomaterials.* 2005;26(1):93–9.
- 642
53. Cui X, Boland T. Human microvasculature fabrication using thermal inkjet printing technol-
643 ogy. *Biomaterials.* 2009;30(31):6221–7.
- 644 54. Boland T, Tao X, Damon BJ, Manley B, Kesari P, Jalota S, et al. Drop-on-demand
645 printing of cells and materials for designer tissue constructs. *Mater Sci Eng: C.*
2007;27(3):372–6.
- 646 55. Nakamura M, Nishiyama Y, Henmi C, Yamaguchi K, Mochizuki S, Koki T, et al. Inkjet
647 bio-
printing as an effective tool for tissue fabrication. *NIP Digital Fabr Conf.* 2006;2006(3):89–
648 92.
56. Nishiyama Y, Nakamura M, Henmi C, Yamaguchi K, Mochizuki S, Nakagawa H, et al. De649 velopment of a three-dimensional bioprinter: construction of cell supporting structures using 650 hydrogel and state-of-the-art inkjet technology. *J Biomech Eng.* 2008;131(3):035001. 651 57. Xu C, Chai W, Huang Y, Markwald RR. Scaffold-free inkjet printing of three-dimensional 652 zigzag cellular tubes. *Biotechnol Bioeng.* 2012;109(12):3152–60.
58. Khatiwala C, Law R, Shepherd B, Dorfman S, Csete M. 3D cell bioprinting for regenerative
653 medicine research and therapies. *Gene Ther Regul.* 2012;07(01):1230004.
- 654 59. Shabnam P, Madhuja G, Frédéric L, Karen CC. Effects of surfactant and gentle
655 agitation on inkjet dispensing of living cells. *Biofabrication.* 2010;2(2):025003.
- 656 60. Chahal D, Ahmadi A, Cheung KC. Improving piezoelectric cell printing accuracy and
reliability through neutral buoyancy of suspensions. *Biotechnol Bioeng.* 2012;109(11):2932–
657 40.
61. Ferris CJ, Gilmore KJ, Beirne S, McCallum D, Wallace GG, In het Panhuis M. Bio-ink for
658 on-demand printing of living cells. *Biomater Sci.* 2013;1(2):224–30.
62. Foty RA, Steinberg MS. The differential adhesion hypothesis: a direct
659 evaluation. *Dev Biol.*
2005;278(1):255–63.
- 660 63. Steinberg MS. Differential adhesion in morphogenesis: a modern view. *Curr Opin Genet*
661 *Dev.* 2007;17(4):281–6.
64. Steinberg MS. Reconstruction of tissues by dissociated cells. Some morphogenetic tissue 662 movements and the sorting out of embryonic cells may have a common explanation. *Science.*
663 1963;141(0036-8075 (Print)):401–8.
- 664 65. Jakab K, Norotte C, Damon B, Marga F, Neagu A, Besch-Williford CL, Kachurin A, et
al. 665 Tissue engineering by self-assembly of cells printed into topologically defined
structures. *666 Tissue Eng.* 2008;14(1937–3341 (Print)):413–21.
- 667 66. Kelm JM, Lorber V, Snedeker JG, Schmidt D, Broggini-Tenzer A, Weisstanner M, et al. A
novel concept for scaffold-free vessel tissue engineering: Self-assembly of microtissue build-
668 ing blocks. *J Biotechnol.* 2010;148(1):46–55.
- 669 67. Gwyther TA, Hu JZ, Christakis AG, Skorinko JK, Shaw SM, Billiar KL, et al. Engineered
670 vascular tissue fabricated from aggregated smooth muscle cells. *Cells Tissues Organs.*
671 2011;194(1):13–24.

68. Adebayo O, Hookway TA, Hu JZ, Billiar KL, Rolle MW. Self-assembled smooth muscle 672 cell tissue rings exhibit greater tensile strength than cell-seeded fibrin or collagen gel rings. *J*
673 *Biomed Mater Res A*. 2013;101 A(2):428–37.
- 674 69. Napolitano AP, Chai P, Dean DM, Morgan JR. Dynamics of the self-assembly of complex
675 cellular aggregates on micromolded nonadhesive hydrogels. *Tissue Eng*. 2007;13(1076–
676 (Print)):2087–94.
- 677 70. Dean DM, Napolitano AP, Youssef J, Morgan JR, Rods, tori, and honeycombs: the di-
678 rected self-assembly of microtissues with prescribed microscale geometries. *FASEB J*.
679 2007;21(14):4005–12.
- 680 71. Khalil S, Nam J, Sun W. Multi-nozzle deposition for construction of 3D biopolymer tissue
681 72. Khalil S, Sun W. Biopolymer deposition for freeform fabrication of hydrogel tissue constructs. *Mater*
682 *Sci Eng: C*. 2007;27(3):469–78.
- 683 73. Smith CM, Christian JJ, Warren WL, Williams SK. Characterizing environmental factors that
684 impact the viability of tissue-engineered constructs fabricated by a direct-write bioassembly 684 tool.
685 *Tissue Eng*. 2007;13(1076–3279 (Print)):373–83.
- 686 74. Smith CM, Stone AL, Parkhill RL, Stewart RI, Simpkins MW, Kachurin AM, Warren WL, 686 et al.
687 Three-dimensional bioassembly tool for generating viable tissue-engineered constructs.
688 *Tissue Eng*. 2004;10(1076–3279 (Print)):1566–76.
- 689 75. Duan B, Hockaday LA, Kang KH, Butcher JT. 3D Bioprinting of heterogeneous aortic valve
690 conduits with alginate/gelatin hydrogels. *J Biomed Mater Res A*. 2012;101 A(5):1255–64.
- 691 76. Hockaday LA, Kang KH, Colangelo NW, Cheung PYC, Duan B, Malone E, et al. Rapid 690 3D
692 printing of anatomically accurate and mechanically heterogeneous aortic valve hydrogel 691 scaffolds.
693 *Biofabrication*. 2012;4(3):035005.
- 694 77. Chang R, Nam J, Sun W. Effects of dispensing pressure and nozzle diameter on cell survival
695 from solid freeform fabrication-based direct cell writing. *Tissue Eng*. 2008;14(1937–3341
696 (Print)):41–8.
- 697 78. Cohen DL, Malone E, Lipson H, Bonassar LJ. Direct freeform fabrication of seeded
698 hydrogels in arbitrary geometries. *Tissue Eng*. 2006;12(1076–3279 (Print)):1325–35.
- 699 79. Christopher MO, Françoise M, Gabor F, Cheryl MH. Biofabrication and testing of a fully cellular
700 nerve graft. *Biofabrication*. 2013;5(4):045007.
- 701 80. Mironov V, Kasyanov V, Markwald RR. Organ printing: from bioprinter to organ
702 biofabrication line. *Curr Opin Biotechnol*. 2011;22(5):667–73.
- 703 81. Norotte C, Marga FS, Niklason LE, Forgacs G. Scaffold-free vascular tissue engineering us700
704 ing bioprinting. *Biomaterials*. 2009;30(30):5910–7.
- 705 82. Kucukgul C, Ozler SB, Inci I, Karakas E, Irmak S, Gozuacik D, et al. 3D bioprinting of 702 biomimetic
706 aortic vascular constructs with self-supporting cells. *Biotechnol Bioeng*.
707 2014;112(4):811–21 n/a-n/a.
- 708 83. Ozler SB, Kucukgul C, Koc B. 3D continuous cell bioprinting. submitted 2015.

UNCORRECTED PROOF

84. Kucukgul C, Ozler B, Karakas HE, Gozuacik D, Koc B. 3D hybrid bioprinting
of macrovas⁷⁰⁵cular structures. *Procedia Eng.* 2013;59(0):183–92.